JOURNAL OF THEORETICAL AND APPLIED MECHANICS
55, 4, pp. 1409-1422, Warsaw 2017
DOI: 10.15632/jtam-pl.55.4.1409

DYNAMIC STABILITY OF A STEPPED DRILLSTRING CONVEYING DRILLING FLUID

Guang-Hui Zhao, Song Tang, Zheng Liang, Ju Li

School of Mechanical Engineering, Southwest Petroleum University, Chengdu 610500, China
e-mail: wy_zgh@126.com; m15102835095@163.com; liangz_2242@126.com; littlemj@126.com

Taking into account differences between a drill pipe (DP) and a drill collar (DC), the drillstring in a vertical well is modeled as a stepped pipe conveying a drilling fluid downwards to the bottom inside the string and then upwards to the ground from the annulus. An analytical model that describes lateral vibration of the drillstring and involves the drillstring gravity, weight on bit (WOB), hydrodynamic force and damping force of the drilling fluid is established. By analysis of complex frequencies, the influences of WOB, borehole diameter, DP length, velocity and density of the drilling fluid on the stability of the system are discussed.

Keywords: drillstring, stepped fluid-conveying pipe, complex frequency, stability, FEM

Nomenclature

A_{ch}	–	cross-sectional flow area of annulus, m^2
A_i	–	cross-sectional flow area inside drillstring, m^2
A_o	–	external cross-sectional area of drillstring, m^2
C_f	–	frictional damping coefficient of drilling fluid
D_{ch}	–	borehole diameter, m
D_h	–	hydraulic diameter of annular flow, m
D_i, D_o	–	inner and outer diameter of drillstring, m
EI	–	flexural rigidity, $N{\cdot}m^2$
k	–	viscous damping coefficient of drilling fluid
L	–	drillstring length, m
M_t	–	mass per unit length of drillstring, kg/m
M_f	–	mass per unit length of fluid inside drillstring, kg/m
p_i	–	fluid pressure inside drillstring, Pa
p_o	–	fluid pressure in annulus, Pa
S_{tot}	–	wetted area per unit length, m^2
T	–	axial force, N
U_i, U_o	–	flow velocity inside and outside drillstring, m/s
ρ_f	–	drilling fluid density, kg/m^3
χ	–	added mass coefficient
ω	–	complex frequency

Subscripts

1 – DP segment, 2 – DC segment, L – at the borehole bottom

1. Introduction

The drillstring is the most widely used and important part of the drilling rig system of petroleum and natural gas. Working under complex conditions, the drillstring is apt to lose stability and collides with the borehole wall seriously. It would lead to reduction in both the quality of wellbore and the service life of drilling tools, and result in the raise of drilling costs ultimately (Hakimi and Moradi, 2010; Zamani *et al.*, 2016; Navarro-López *et al.*, 2007).

In the recent years, many researches on transverse vibration of the drillstring have been conducted. But most of these works ignored the interaction between the drillstring and drilling mud. The conventional exploitation mode of oil and gas reservoir is through the vertical well, and the studies on dynamic characteristics of the drillstring in the vertical well are the most. The influence of installation sites of stabilizers on lateral vibration of the drillstring was discussed by Zhao *et al.* (2014) and Mongkolcheep *et al.* (2015). Considering the damping effect of the drilling fluid, Ghasemloonia *et al.* (2013, 2014) analyzed the coupled axial-transverse vibration of the drillstring in vibration-assisted rotary drilling, however the flow effect was not included. With the widespread implementation of extended reach wells in offshore and onshore oilfields, the dynamic characteristics of drillstrings in the horizontal and inclined wells also attract attention of the researchers. Considering the drillstring in an inclined well as a simply supported axially moving rotor, Sahebkar *et al.* (2011) derived the kinetic equation of the string by means of Hamilton's principle. Zhu and Di (2011) and Zhu *et al.* (2012) studied the effect of pre-bent deflection on lateral vibration of drill collars in horizontal and inclined wells respectively. Tikhonov and Safronov (2011) and Samuel and Yao (2013) developed a two-dimensional transverse vibration model of the drillstring to three-dimensional circumstances. Because of the complexity of the drillstring system, the influence of drilling fluid flow on the dynamic response of the drillstring was not considered in these studies.

With the whole process of drilling operation, both the hollow drillstring and the annular space between the drillstring and borehole wall are filled with a drilling fluid flowing axially. The drillstring could be regarded as a flexible and slender pipe conveying fluid in the wellbore. Fluid-solid coupling vibration of the fluid-conveying pipe has attracted considerable attention for its extensive engineering applications and rich dynamic responses (Jin and Song, 2005; Xu and Yang, 2006; Panda and Kar, 2007; Wang, 2009; Ni *et al.*, 2015). As early as 1978, Hannoyer and Paidoussis (1978) established a dynamic model of tubular beams simultaneously subjected to internal and external axial flows based on dynamics of cylindrical structures subjected to axial flow (Paidoussis, 1973). Later, Zhang and Miska (2005) reduced the drillstring to a uniform tubular beam, and used the model of fluid-conveying pipe to simulate the dynamic stability of the drillstring system in response to its own weight, WOB and drilling fluid flowing inside and outside the string. In 2008, Paidoussis *et al.* (2008) revised the expression of the frictional viscous force in the normal direction due to the external flow used in the previous studies (Luu, 1983), and discussed the effect of flow velocity on the stability of the drillstring-like system with a floating drill bit by using Galerkin-Fourier method. Meanwhile, Qian *et al.* (2008) studied dynamics of the drill-string-like system in the counterflush drilling process where the drilling fluid flowed downwards to the bottom through the annular region and returned upwards to the ground in the drillstring. The model of the fluid-conveying pipe could reflect the characteristics of fluid-structure interaction of the string system well, which was validated by an experiment (Rinaldi and Paidoussis, 2012). In these analytical models, however, the drillstring was reduced to a uniform pipe that was very different from the actual drillstring. The drillstring is mainly composed of DP and DC. Compared with DP, DC has larger outer diameter and smaller inner diameter which makes both the line density and stiffness of DC much larger than those of DP. Under a given drilling pressure, the dynamic prediction of the uniform string model, whose

neutral point (the point where the axial force is zero) is much higher than that of the actual drillstring, may be inaccurate.

In view of the complexity and diversity of make-up of the string, well path, drilling fluid properties and drilling parameters, it is still impossible to describe the dynamic response of the drillstring system quantitatively. At present, it remains the main way to explore the effect of a single factor on the system and coupling interaction among several factors. The present study is concerned with the dynamics of the drillstring that is in a vertical well and simplified to be a stepped fluid-conveying pipe composed of DP and DC. Considering the drillstring gravity, WOB and drilling fluid flowing inside and outside the string, an analytical model of lateral vibration of drillstring is proposed. The effect of the fluid-pipe interaction and the drillstring structure on the stability of the drillstring system is discussed.

2. Dynamic model

The drillstring that is composed of DP, DC, connector and a variety of accessories plays an important role in conveying drilling fluid, exerting WOB and transmitting power on the bit. In the drilling process using a PDC bit or an impregnated diamond bit, the bottom hole rock is broken by cutting or grinding. So, WOB fluctuates weakly and could be reduced to a constant value. Under the action of drilling pressure and floating weight, the upper part of the drillstring is subjected to tensile stress and the lower part is compressed. To avoid the DP from buckling, the neutral point is generally located at the section of DC. Generally, the drilling fluid is pumped downwards through the inner channel of the drillstring from the well head, flows through the drill bit and returns to the ground along the annular space between the drillstring and borehole wall. Ignoring the influence of tool joints and flexibility of the drilling rig, the drillstring is simplified to be a stepped fluid-conveying pipe composed of DP and DC, which is constrained by a fixed hinge at the well head and a movable hinge at the bottom hole (Fig. 1). The origin of the

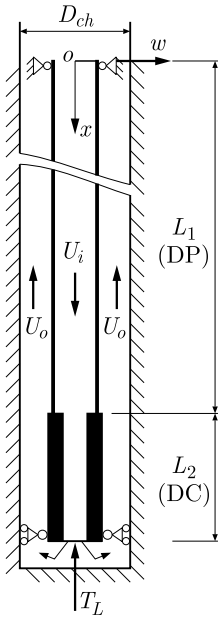

Fig. 1. Sketh of drillstring

coordinate o is located at the well head, x-axis is directed vertically downwards, and the lateral displacement of the drillstring is $w(x,t)$. Considering the drillstring gravity, WOB, constraint of the wellbore and drilling fluid flowing inside and outside the drillstring, the equation of lateral

vibration of the stepped drillstring could be established by doing similar element analysis as the model of Paidoussis *et al.* (2008)

$$\begin{aligned} &EI\frac{\partial^4 w}{\partial x^4}+M_t\frac{\partial^2 w}{\partial t^2}+M_f\Big(\frac{\partial^2 w}{\partial t^2}+2U_i\frac{\partial^2 w}{\partial t\partial x}+U_i^2\frac{\partial^2 w}{\partial x^2}\Big)\\ &\quad+\chi\rho_f A_o\Big(\frac{\partial^2 w}{\partial t^2}-2U_o\frac{\partial^2 w}{\partial t\partial x}+U_o^2\frac{\partial^2 w}{\partial x^2}\Big)-\frac{\partial}{\partial x}(A_o p_o-A_i p_i-T)\frac{\partial w}{\partial x}\\ &\quad-(A_o p_o-A_i p_i-T)\frac{\partial^2 w}{\partial x^2}+\frac{1}{2}C_f\rho_f D_o U_o\frac{\partial w}{\partial t}+k\frac{\partial w}{\partial t}=0 \end{aligned} \tag{2.1}$$

where

$$\chi=\frac{D_{ch}^2+D_o^2}{D_{ch}^2-D_o^2}\qquad D_h=\frac{4A_{ch}}{S_{tot}}\qquad S_{tot}=\pi(D_{ch}+D_o)$$

$$k=\sqrt{2\nu\omega}\pi\rho_f D_o\left(1+\frac{(D_{ch}/D_o)^3}{[1-(D_{ch}/D_o)^2]^2}\right)$$

(symbolic meaning are listed in nomenclature), and

$$\frac{\partial}{\partial x}(A_o p_o-A_i p_i-T)=-[M_t-\rho_f(A_o-A_i)+M_f-\rho_f A_o]g+\frac{1}{2}C_f\rho_f D_o U_o^2\Big(1+\frac{D_o}{D_h}\Big) \tag{2.2}$$

The differences between Eq. (2.1) and the model of the drillstring-like system of Paidoussis *et al.* (2008) are mainly in two aspects: 1) except for the friction damping C_f and density ρ_f, all the physical parameters are different between the DP part and DC part; 2) WOB that is an important factor in the stability of the drillstring is included and the drill bit is constrained by a movable hinge. So, the present model and parameters are more closely related to a real system. In the following equations, subscripts 1 and 2 would be used to indicate the parameters associated with DP and DC, respectively. The term $(A_o p_o - A_i p_i - T)$ in Eq. (2.1) could be obtained by integrating Eq. (2.2) as follows.

For the DP segment

$$\begin{aligned} A_o p_o-A_i p_i-T&=A_{o2}p_{oL}-A_{i2}p_{iL}-T_L\\ &+\Big\{[M_{t2}-\rho_f(A_{o2}-A_{i2})+M_{f2}-\rho_f A_{o2}]g-\frac{1}{2}C_f\rho_f D_{o2}U_{o2}^2\Big(1+\frac{D_{o2}}{D_{h2}}\Big)\Big\}(L-L_1)\\ &+\Big\{[M_{t1}-\rho_f(A_{o1}-A_{i1})+M_{f1}-\rho_f A_{o1}]g-\frac{1}{2}C_f\rho_f D_{o1}U_{o1}^2\Big(1+\frac{D_{o1}}{D_{h1}}\Big)\Big\}(L_1-x) \end{aligned} \tag{2.3}$$

And for the DC segment

$$\begin{aligned} A_o p_o-A_i p_i-T&=A_{o2}p_{oL}-A_{i2}p_{iL}-T_L\\ &+\Big\{[M_{t2}-\rho_f(A_{o2}-A_{i2})+M_{f2}-A_{o2}\rho_f]g-\frac{1}{2}C_f\rho_f D_{o2}U_{o2}^2\Big(1+\frac{D_{o2}}{D_{h2}}\Big)\Big\}(L-x) \end{aligned} \tag{2.4}$$

where p_{iL} and p_{oL} are fluid pressures of the bottom hole inside and outside the drillstring, respectively. They could be calculated based on the following assumptions: fluid pressure in the annulus is zero at the well head, namely, $p_o\big|_{x=0}=0$; the local loss near the joint of DP and DC is ignored, and the variation of pressure p_o with x is approximated as a piecewise linear function. Considering the pressure drop of the drilling fluid flowing through the bit jet (Zhang *et al.*, 2005), one obtains

$$\begin{aligned} p_{oL}&=\rho_f gL+\frac{1}{2A_{o2}}C_f D_{o2}U_{o2}^2(L-L_1)\frac{D_{o2}}{D_{h2}}+\frac{1}{2A_{o1}}C_f D_{o1}U_{o1}^2L_1\frac{D_{o1}}{D_{h1}}\\ p_{iL}&=p_{oL}+\rho_f U_{o2}(U_{o2}-U_{i2}) \end{aligned} \tag{2.5}$$

Substituting Eqs. (2.2)-(2.5) into Eq. (2.1), the equations of lateral vibration of DP and DC could be obtained. The boundary conditions at the well head and bottom are

$$w(0,t)=\frac{\partial^2 w}{\partial x^2}(0,t)=0 \qquad w(L,t)=\frac{\partial^2 w}{\partial x^2}(L,t)=0 \tag{2.6}$$

For convenience of the analysis, the following dimensionless quantities could be defined based on the parameters of DC

$$\eta=\frac{w}{L} \qquad \xi=\frac{x}{L} \qquad \tau=\frac{t}{L^2}\sqrt{\frac{E_2I_2}{M_{t2}+M_{f2}+\rho_f A_{o2}}} \qquad u_{i1}=\sqrt{\frac{M_{f1}}{E_2I_2}}U_{i1}L$$

$$u_{i2}=\sqrt{\frac{M_{f2}}{E_2I_2}}U_{i2}L \qquad u_{o1}=\sqrt{\frac{\rho_f A_{o1}}{E_2I_2}}U_{o1}L \qquad u_{o2}=\sqrt{\frac{\rho_f A_{o2}}{E_2I_2}}U_{o2}L$$

$$\beta_{i1}=\frac{M_{f1}}{M_{t2}+M_{f2}+\rho_f A_{o2}} \qquad \beta_{o1}=\frac{\rho_f A_{o1}}{M_{t2}+M_{f2}+\rho_f A_{o2}}$$

$$\beta_{i2}=\frac{M_{f2}}{M_{t2}+M_{f2}+\rho_f A_{o2}} \qquad \beta_{o2}=\frac{\rho_f A_{o2}}{M_{t2}+M_{f2}+\rho_f A_{o2}}$$

$$\gamma_1=\frac{[M_{t1}-\rho_f(A_{o1}-A_{i1})+M_{f1}-A_{o1}\rho_f]gL^2}{E_2I_2} \qquad \kappa_1=\frac{k_1L^2}{\sqrt{E_2I_2(M_{t2}+M_{f2}+\rho_f A_{o2})}}$$

$$\gamma_2=\frac{[M_{t2}-\rho_f(A_{o2}-A_{i2})+M_{f2}-A_{o2}\rho_f]gL^2}{E_2I_2} \qquad \kappa_2=\frac{k_2L^2}{\sqrt{E_2I_2(M_{t2}+M_{f2}+\rho_f A_{o2})}}$$

$$\Gamma=\frac{L^2T_L}{E_2I_2} \qquad \Pi_i=\frac{L^2A_{f2}p_{iL2}}{E_2I_2} \qquad \Pi_o=\frac{L^2A_{o2}p_{oL}}{E_2I_2} \qquad c_f=\frac{4C_f}{\pi}$$

$$h_1=\frac{D_{o1}}{D_{h1}} \qquad h_2=\frac{D_{o2}}{D_{h2}} \qquad \varepsilon_1=\frac{L}{D_{o1}} \qquad \varepsilon_2=\frac{L}{D_{o2}} \qquad \lambda=\frac{A_{o1}}{A_{o2}}$$

$$\alpha_1=\frac{E_1I_1}{E_2I_2} \qquad \alpha_2=\frac{M_{t1}+M_{f1}+\rho_f A_{o1}}{M_{t2}+M_{f2}+\rho_f A_{o2}} \qquad \delta=\frac{L_1}{L}$$

By substituting the quantities above into Eq. (2.1), the dimensionless governing equations for DP and DC are obtained, respectively. For the DP segment

$$\begin{aligned}
&\alpha_1\frac{\partial^4\eta}{\partial\xi^4}+[\alpha_2+\beta_{o1}(\chi_1-1)]\frac{\partial^2\eta}{\partial\tau^2}+2\Big(\sqrt{\beta_{i1}}u_{i1}-\chi_1\sqrt{\beta_{o1}}u_{o1}\Big)\frac{\partial^2\eta}{\partial\tau\partial\xi}+\Big(u_{i1}^2+\chi_1u_{o1}^2\Big)\frac{\partial^2\eta}{\partial\xi^2}\\
&\quad-\Big\{-\Gamma-\Pi_{iL}+\Pi_{oL}+\Big[\gamma_2-\frac{1}{2}c_f\varepsilon_2u_{o2}^2(1+h_2)](1-\delta)\\
&\quad+\Big[\gamma_1-\frac{1}{2}c_f\varepsilon_1u_{o1}^2(1+h_1)\Big](\delta-\xi)\Big\}\frac{\partial^2\eta}{\partial\xi^2}+\Big[\gamma_1-\frac{1}{2}c_f\varepsilon_1u_{o1}^2(1+h_1)\Big]\frac{\partial\eta}{\partial\xi}\\
&\quad+\frac{1}{2}c_f\varepsilon_1\sqrt{\beta_{o1}}u_{o1}\frac{\partial\eta}{\partial\tau}+\kappa_1\frac{\partial\eta}{\partial\tau}=0
\end{aligned} \tag{2.7}$$

and for the DC segment

$$\begin{aligned}
&\frac{\partial^4\eta}{\partial\xi^4}+[1+\beta_{o2}(\chi_2-1)]\frac{\partial^2\eta}{\partial\tau^2}+2\Big(\sqrt{\beta_{i2}}u_{i2}-\chi_2\sqrt{\beta_{o2}}u_{o2}\Big)\frac{\partial^2\eta}{\partial\xi\partial\tau}+(u_{i2}^2+\chi_2u_{o2}^2)\frac{\partial^2\eta}{\partial\xi^2}\\
&\quad-\Big\{-\Gamma-\Pi_{iL}+\Pi_{oL}+\Big[\gamma_2-\frac{1}{2}c_f\varepsilon_2u_{o2}^2(1+h_2)\Big](1-\xi)\Big\}\frac{\partial^2\eta}{\partial\xi^2}\\
&\quad+\Big[\gamma_2-\frac{1}{2}c_f\varepsilon_2u_{o2}^2(1+h_2)\Big]\frac{\partial\eta}{\partial\xi}+\frac{1}{2}c_f\varepsilon_2u_{o2}\sqrt{\beta_{o2}}\frac{\partial\eta}{\partial\tau}+\kappa_2\frac{\partial\eta}{\tau}=0
\end{aligned} \tag{2.8}$$

where

$$\begin{aligned} \Pi_{oL} &= \frac{A_{o2}\rho_f g L^3}{E_2 I_2} + \frac{1}{2}c_f \varepsilon_2 u_{o2}^2 (1-\delta) h_2 + \frac{1}{2}c_f \varepsilon_1 u_{o1}^2 \delta\lambda h_1 \\ \Pi_{iL} &= \alpha^2 \Pi_{oL} + \alpha u_{o2}(\alpha u_{o2} - u_{i2}) \end{aligned} \tag{2.9}$$

The dimensionless boundary conditions are

$$\eta(0,\tau) = \frac{\partial^2 \eta}{\partial \xi^2}(0,\tau) = 0 \qquad \eta(1,\tau) = \frac{\partial^2 \eta}{\partial \xi^2}(1,\tau) = 0 \tag{2.10}$$

3. Method of solution

It is difficult to solve Eqs. (2.7)-(2.10) of the stepped fluid-conveying pipe by means of the conventional Galerkin method, the multiple scales method and the differential quadrature method. Here, the finite element method that takes the Hermite polynomial as shape function is used.

3.1. The finite element method

The drillstring is divided into n elements by $(n+1)$ nodes. The length of the j-th element is $L_j = \xi_{j+1} - \xi_j$, and the lateral displacement $\eta(\xi)$ is represented by means of cubic Hermite interpolation

$$\eta(\xi) = \mathbf{N}_{ej} \cdot \boldsymbol{\eta}_{ej} \qquad \xi_j \leqslant \xi \leqslant \xi_{j+1} \tag{3.1}$$

where $\mathbf{N}_{ej}$ and $\boldsymbol{\eta}_{ej}$ are primary functions and nodal displacements of the j-th element, respectively, and denoted as

$$\mathbf{N}_{ej} = \begin{bmatrix} \lambda_j^2(\lambda_j + 3\lambda_{j+1}) \\ L_j \lambda_j^2 \lambda_{j+1} \\ \lambda_{j+1}^2(\lambda_{j+1} + 3\lambda_j) \\ -L_j \lambda_{j+1}^2 \lambda_j \end{bmatrix}^{\mathrm{T}} \qquad \boldsymbol{\eta}_{ej} = \begin{bmatrix} \eta_j \\ \varphi_j \\ \eta_{j+1} \\ \varphi_{j+1} \end{bmatrix}$$

where $\lambda_j = (\xi_{j+1} - \xi)/L_j$, $\lambda_{j+1} = (\xi - \xi_j)/L_j$. η_j and φ_j are deflection and rotation angles of the j-th node, respectively. Substituting Eq. (3.1) into Eqs. (2.7)-(2.8) and using the virtual work principle, we obtain the equation of motion of the j-th element as follows

$$\mathbf{M}_{ej}\ddot{\boldsymbol{\eta}}_{ej} + \mathbf{C}_{ej}\dot{\boldsymbol{\eta}}_{ej} + \mathbf{K}_{ej}\boldsymbol{\eta}_{ej} = \mathbf{0} \tag{3.2}$$

where $\mathbf{M}_{ej}$, $\mathbf{C}_{ej}$, and $\mathbf{K}_{ej}$ are the mass matrix, damping matrix and stiffness matrix of the j-th element, respectively. It should be noted that the element matrices of DP are different from those of DC.

Assembling the element matrices in the global coordinate system and using boundary conditions (2.10), the finite element equation of the whole drillstring system could be obtained

$$\mathbf{M}\ddot{\boldsymbol{\eta}} + \mathbf{C}\dot{\boldsymbol{\eta}} + \mathbf{K}\boldsymbol{\eta} = \mathbf{0} \tag{3.3}$$

where $\mathbf{M}$, $\mathbf{C}$ and $\mathbf{K}$ are all global matrices of the order $2n$ corresponding to mass, damping and stiffness, respectively.

The solutions to Eq. (3.3) could be expressed as

$$\boldsymbol{\eta} = \overline{\boldsymbol{\eta}} \mathrm{e}^{\omega\tau} \tag{3.4}$$

Substituting it into Eq. (3.3), gives

$$(\omega^2\mathbf{M}+\omega\mathbf{C}+\mathbf{K})\overline{\boldsymbol{\eta}}=\mathbf{0} \tag{3.5}$$

Equation (3.5) is a generalized eigenvalue problem, and the stability of the drillstring system could be determined by calculating the complex eigenvalues ω of the matrix $\mathbf{E}$

$$\mathbf{E}=\begin{bmatrix}\mathbf{0} & \mathbf{I}\\ -\mathbf{M}^{-1}\mathbf{K} & -\mathbf{M}^{-1}\mathbf{C}\end{bmatrix} \tag{3.6}$$

$\mathrm{Re}(\omega)$ and $\mathrm{Im}(\omega)$ are the real and imaginary parts of ω, respectively. $\mathrm{Re}(\omega)$ is related to modal damping of the system, and $\mathrm{Im}(\omega)$ is the natural frequency. In the case of $\mathrm{Re}(\omega)\geqslant 0$ and $\mathrm{Im}(\omega)\neq 0$ flutter instability occurs, and the fluid velocity at which $\mathrm{Re}(\omega)$ increases to zero from negative values is called the critical flutter velocity u_{cf}. Buckling instability happens when $\mathrm{Im}(\omega)=0$, and the corresponding flow rate is the critical buckling velocity u_{cd}. In this paper, u_{cf} and u_{cd} are all defined based on the internal flow of the DP segment.

3.2. Model validation

The correctness of the finite element method and the numerical model is verified by comparing the present results with those given by Dai *et al.* (2013) and Paidoussis *et al.* (2008).

Firstly, the present model is reduced into a fluid-conveying cantilevered pipe that consists of an aluminum segment and a steel segment according to Dai *et al.* (2013). These two segments have the same cross section and length, and the end of the aluminum segment is fixed. For the cantilever beam, the rows and columns that are associated with the fixed end in the global matrices of the present model are set to zero. The evolution of the first four complex frequencies with the flow velocity is illustrated in Fig. 2. The dimensionless critical flutter velocity of the second mode is $u_{cf}=7.8$, which is completely consistent with literature (Dai *et al.*, 2013), and shows correctness of the finite element method.

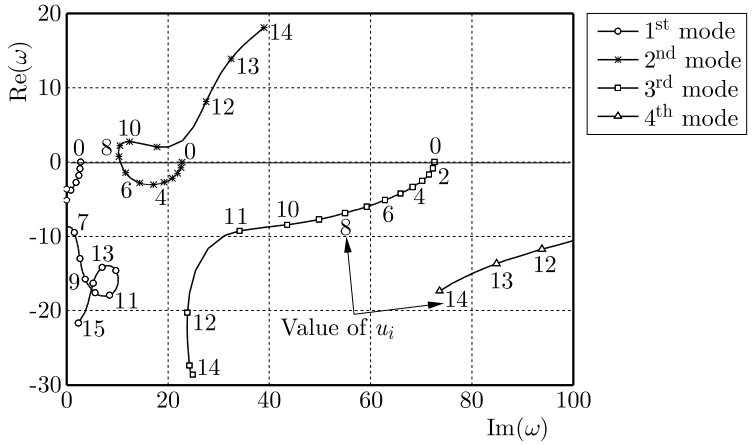

Fig. 2. The present result of the first four dimensionless complex frequencies as functions of u_i

Secondly, in accordance with Paidoussis *et al.* (2008), the stepped pipe is reduced to a uniform tubular column and the parameters are: $L_1=0\,\mathrm{m}$, $L_2=1000\,\mathrm{m}$, $D_{i2}=0.45\,\mathrm{m}$, $D_{o2}=0.5\,\mathrm{m}$, $D_{ch}=10\,\mathrm{m}$, $\rho_f=998\,\mathrm{kg/m^3}$, $\rho_t=7830\,\mathrm{kg/m^3}$, $C_f=0.0125$, and $\nu=10^{-6}\,\mathrm{m^2/s}$. By using the finite element method, we obtain the first three complex frequencies varying with the flow rate u_i (Fig. 3). This result can be compared to that given by Paidoussis *et al.* (2008) through the hybrid Galerkin-Fourier method. It needs to be pointed out that the definition of ω in this literature is different from that in the present paper. Denoting ω in Paidoussis *et al.* (2008) as ω^*,

the relationships between ω^* and ω in this paper are: $\mathrm{Re}(\omega^*) = \mathrm{Im}(\omega)$ and $\mathrm{Im}(\omega^*) = -\mathrm{Re}(\omega)$. As shown in Fig. 3, the present results agree with those of Paidoussis *et al.* (2008) very well, and the dimensionless critical flutter velocity of the second and third modes are $u_{cf} = 2.2$ and $u_{cf} = 2.56$, respectively. Compared with the result of Paidoussis *et al.* (2008), the relative errors are only 3.8% and 0.4%. It demonstrates correctness of the present model. So, the present model and algorithm would be used to analyze the stability of the stepped drillstring system composed of DP and DC.

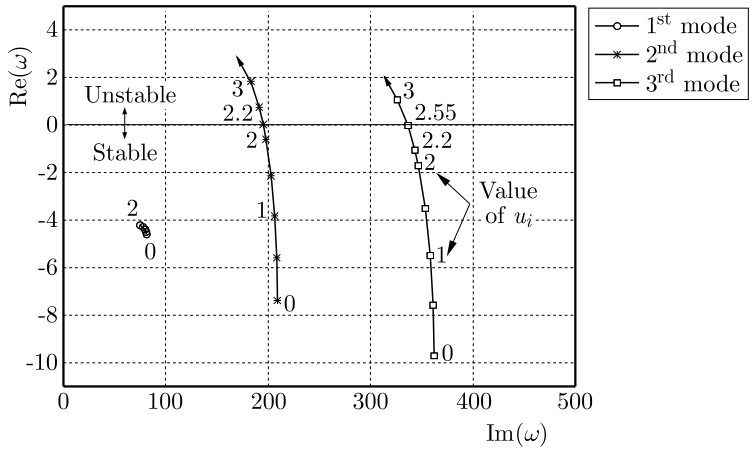

Fig. 3. The first three complex frequencies as functions of the velocity of fluid u_i

4. Dynamic stability of drillstring system

The drillstring system in the vertical well with well depth $L = 1000\,\mathrm{m}$ is studied. The parameters are, for DP: $L_1 = 948\,\mathrm{m}$, $D_{i1} = 0.127\,\mathrm{m}$, $D_{o1} = 0.1016\,\mathrm{m}$, $m_{t1} = 43.75\,\mathrm{kg/m}$; and for DC: $L_2 = 52\,\mathrm{m}$, $D_{i2} = 0.203\,\mathrm{m}$, $D_{o2} = 0.07144\,\mathrm{m}$, $m_{t2} = 228.28\,\mathrm{kg/m}$; in addition, $T = 50\,\mathrm{kN}$, $D_{ch} = 0.314\,\mathrm{m}$, $\rho_f = 1200\,\mathrm{kg/m^3}$, $\nu = 10^{-6}\,\mathrm{m^2/s}$. The viscosity damping coefficient C_f of the drilling fluid is a semi-empirical value of 0.0125, and k could be calculated iteratively for each natural frequency.

Figure 4 illustrates the first four complex frequencies of this DP-DC system varying with the flow rate U_{i1}, and indicates that the system is in the stable state for $U_{i1} \leqslant 110\,\mathrm{m/s}$. With an increase in U_{i1}, $\mathrm{Re}(\omega)$ and $\mathrm{Im}(\omega)$ all decrease gradually, and stability of the DP-DC system deteriorates.

In order to show the difference between the present stepped model and the uniform column model (Zhang and Miska, 2005), the drillstring is also simplified as a uniform DP model, i.e. $L_1 = 1000\,\mathrm{m}$, $L_2 = 0$, the other parameters are chosen as the DP-DC model above. For this DP model, the first four complex frequencies ω that are functions of U_{i1} are obtained and shown in Fig. 5. The system loses stability by buckling in its first mode at $U_{i1} = 43.7\,\mathrm{m/s}$, namely, $u_{cd} = 43.7\,\mathrm{m/s}$.

By comparing Fig. 5 to Fig. 4, one could find that the stability characteristics of these two models are very different. Both natural frequency and critical buckling velocity of the stepped DP-DC model are all much higher than those given by the uniform DP model. Compared with DP model, DP-DC model has a lower neutral point and a higher stiffness of the compression section because the linear density and stiffness of DC are all larger than those of DP. This is consistent with the realistic well condition. As a result, DC could improve the stability of the drillstring system significantly, and the stepped DP-DC model could describe the stability of the drillstring system better.

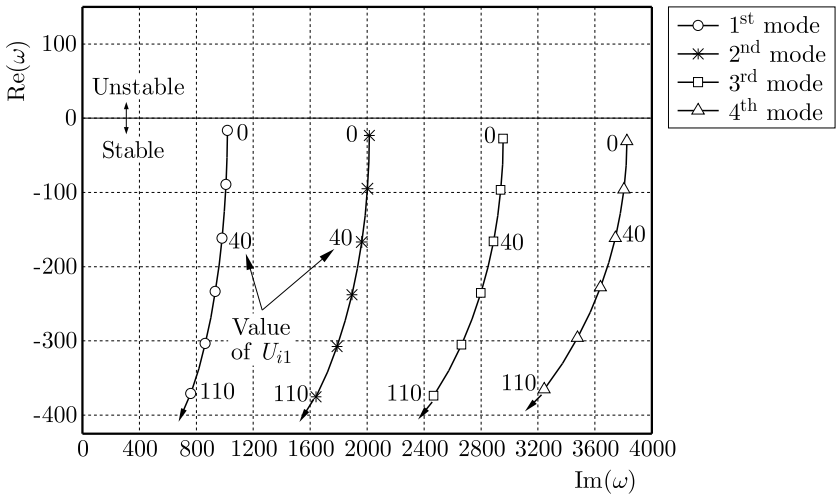

Fig. 4. The first four complex frequencies as functions of U_{i1} by the stepped DP-DC model ($D_{ch} = 0.314\,\mathrm{m}$)

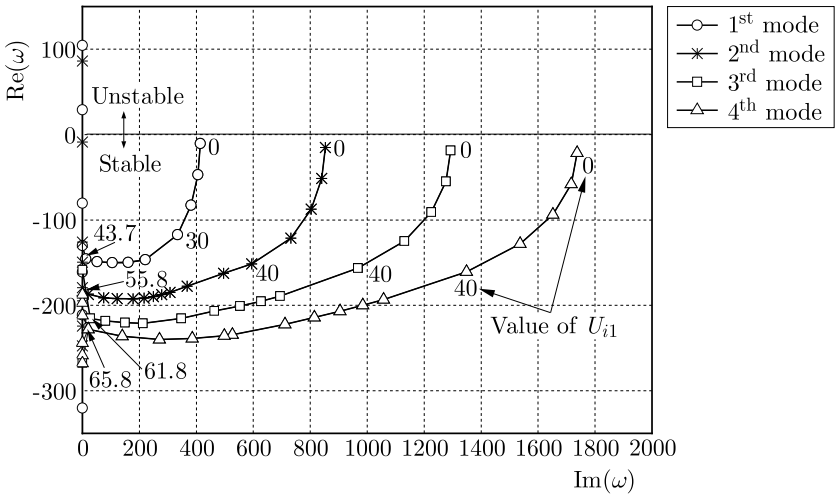

Fig. 5. The first four complex frequencies as functions of U_{i1} by the uniform DP model

5. The effect of parameters on stability

In addition to the internal flow rate U_i, the parameters such as WOB T_L, borehole size D_{ch}, well depth L and drilling fluid density ρ_f also have effects on the stability of the drillstring system.

5.1. WOB

WOB is an important drilling parameter which influences drilling speed greatly and could be controlled by adjusting the hook load. With an increase in WOB, the neutral point gradually moves up. In order to avoid the DP from compression, the neutral point should be located in the drill collar. As a result, WOB should not exceed 98kN for the drillstring system at hand. Figure 6 shows the variation of the first four dimensionless complex frequencies with WOB (T_L) for $U_{i1} = 5\,\mathrm{m/s}$. It means that the drillstring system is stable under the normal drilling condition ($T_L \leqslant 98\,\mathrm{kN}$). Along with T_L increasing, $\mathrm{Re}(\omega)$ increases and $\mathrm{Im}(\omega)$ decreases. It means that WOB is the instability drive of the drillstring system. As the WOB increases further, the buckling instability will occur eventually.

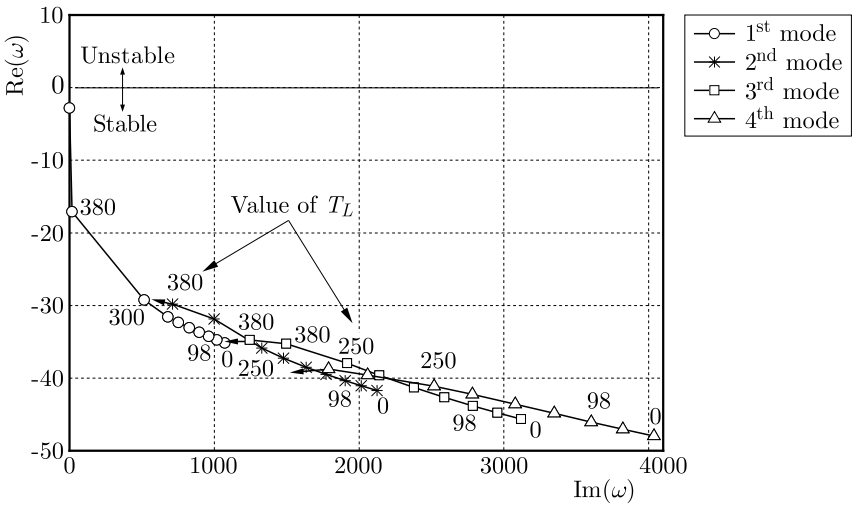

Fig. 6. The first four dimensionless complex frequencies as functions of T_L at $U_{i1} = 5\,\mathrm{m/s}$

5.2. Borehole size

Borehole diameter D_{ch} can be approximated to the bit diameter. In order to ensure implement of wash over fishing operation, 8-in (0.203 m) DC should be equipped with the bit not smaller than 91/2-in (0.2413 m) (NDRC, 2007). The borehole size affects the annular flow velocity. Under the conditions of $D_{ch} = 0.2669\,\mathrm{m}$, 0.2413 m and 0.314 m, the variation of complex frequencies of the drillstring with fluid velocity of U_{i1} are obtained and shown in Fig. 4, Fig. 7 and Fig. 8, respectively. It could be concluded by comparative analysis of these three cases that: Im(ω) of the first four modes decreases along with increasing U_{i1}; the critical buckling velocity (u_{cd}) exceeds 110 m/s for $D_{ch} = 0.314\,\mathrm{m}$ (as shown in Fig. 4), $u_{cd} = 102.2\,\mathrm{m/s}$ for $D_{ch} = 0.2669\,\mathrm{m}$ (Fig. 7) and $u_{cd} = 70.9\,\mathrm{m/s}$ for $D_{ch} = 0.2413\,\mathrm{m}$ (Fig. 8), respectively. It is shown that the drillstring system is more stable for the wellbore with larger size. Therefore, an increase in the fluid velocity, both inside and outside the drillstring, will drive the drillstring system buckling instability.

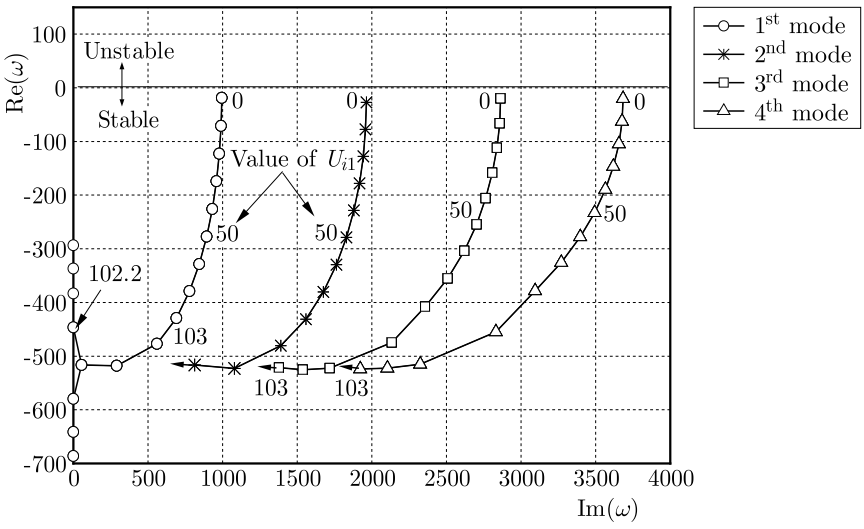

Fig. 7. The first four complex frequencies as functions of U_i for $D_{ch} = 0.2669\,\mathrm{m}$

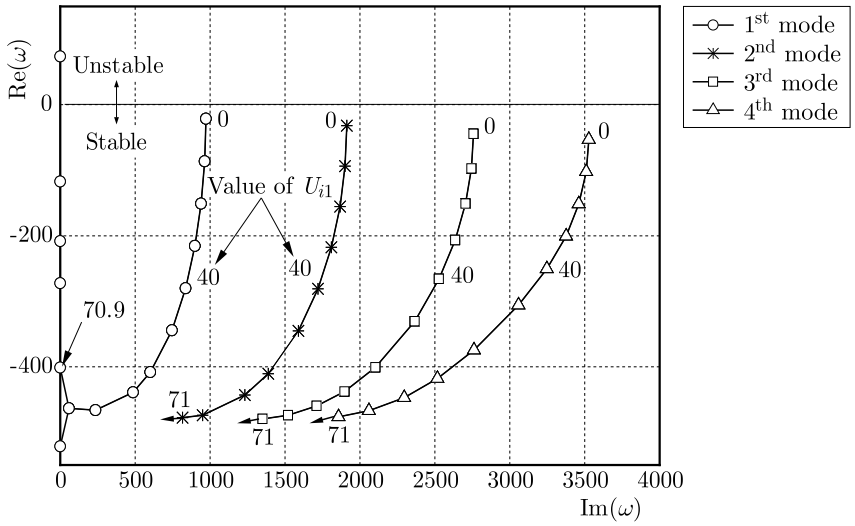

Fig. 8. The first four complex frequencies as functions of U_i for $D_{ch} = 0.2413\,\mathrm{m}$

5.3. Drillstring length

In the actual drilling operation, the structure and length of DC are determined according to the design WOB and remain constant, while length of DP increases in the drilling process. Keeping $L_2 = 52\,\mathrm{m}$, $\mathrm{Im}(\omega)$ of the first four modes that varies along with length of the drillstring is illustrated in Fig. 9. It shows that the relationship between $\mathrm{Im}(\omega)$ and L is similar to a parabola. As the well depth increases, the stability of the drillstring system becomes worse, but the effect of the drillstring length on the stability is smaller and smaller.

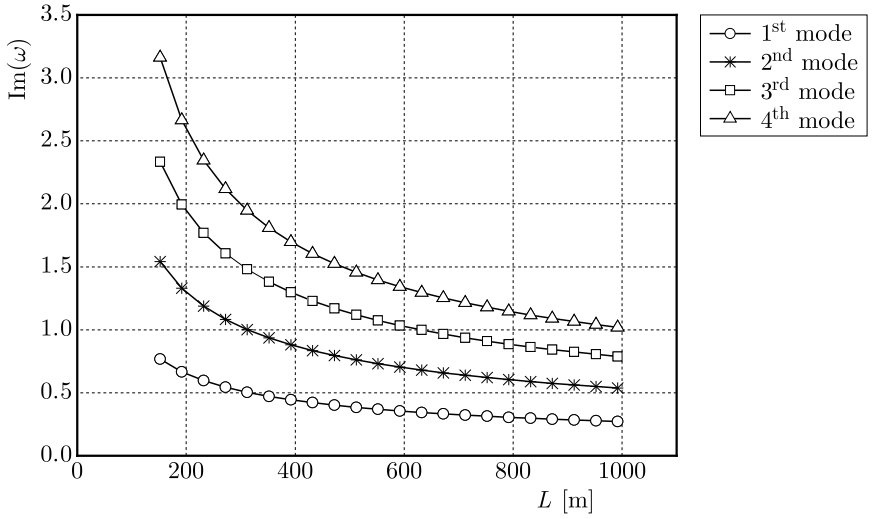

Fig. 9. The effect of the drillstring length on natural frequencies

5.4. Drilling fluid density

In addition to carrying cuttings, cooling and lubricating bit, the drilling fluid plays important roles in stabilizing the borehole wall and balancing the formation pressure. The formation pressure is changing with the drilling depth and needs to be balanced by adjusting the drilling fluid density. The density ρ_f exerts influence on its hydrodynamic characteristic and the buoyant weight of drillstring. Varying ρ_f from $800\,\mathrm{kg/m^3}$ to $1800\,\mathrm{kg/m^3}$, the first four natural

frequencies are shown in Fig. 10. With an increase in ρ_f, the natural frequencies of the system increase slightly, and the stability improves in a minor way.

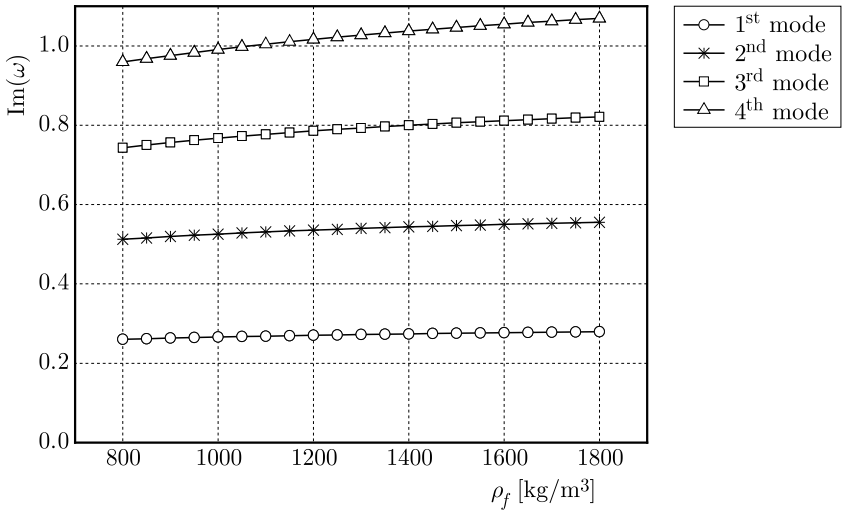

Fig. 10. The effect of drilling fluid density on natural frequencies

6. Conclusion

The drillstring in a vertical well is reduced to a stepped fluid-conveying pipe composed of DP segment and DC segment. Considering the interaction among drillstring gravity, WOB, and drilling fluid that flows inside and outside the drillstring, we propose an analytical model of lateral vibration of the drillstring, discuss the dynamic stability by means of complex frequencies and come to the following conclusions:

- The DC segment whose linear density and stiffness are much larger than that of the DP, could improve the drillstring stability significantly and has a great effect on the dynamics of the whole system. Compared with the uniform string model, the stepped DP-DC model could reflect the dynamic characteristics of the drillstring system better.
- Both WOB and delivery capacity are sources of instability in the drillstring system, and they have a significant effect on the stability of the drillstring system. Buckling instability occurs eventually as these two parameters increase further.
- Along with the increasing well depth, natural frequencies decrease parabolically and the drillstring stability becomes worse. But this influence is smaller and smaller with an increase in the drilling depth.
- Drilling fluid density has a positive effect on the drillstring stability, yet in a minor way.

In the course of drilling operation, one could improve the dynamic stability of the drillstring system by taking actions such as increasing the DC length properly, optimizing the structure of BHA, reducing flow rate under the condition of ensuring cuttings carrying, adopting underbalanced drilling technology, and so on. With the development of logging-while-drilling and controlling technology, the dynamics of drillstring systems with feedback control may be the focus of research in the future.

Acknowledgments

This project was supported by the Open Fund (OGE201403-10) of Key Laboratory of Oil and Gas Equipment, Ministry of Education (SWPU), and the National Natural Science Foundation (51134004) and CSC of China. We also acknowledge association with UNSW.

References

1. Chen S.L., Geradin M., 1995, An improved transfer matrix technique as applied to BHA lateral vibration analysis, *Journal of Sound and Vibration*, **185**, 1, 93-106
2. Dai H.L., Wang L., Ni Q., 2013, Dynamics of a fluid-conveying pipe composed of two different materials, *International Journal of Engineering Science*, **73**, 67-76
3. Ghasemloonia A., Geoff Rideout D., Butt S.D., 2013, Vibration analysis of a drillstring in vibration-assisted rotary drilling: finite element modeling with analytical validation, *Journal of Energy Resources Technology*, **135**, 3, 1-18
4. Ghasemloonia A., Geoff Rideout D., Butt S.D., 2014, Analysis of multi-mode nonlinear coupled axial-transverse drillstring vibration in vibration assisted rotary drilling, *Journal of Petroleum Science and Engineering*, **116**, 36-49
5. Hakimi H., Moradi S., 2010, Drillstring vibration analysis using differential quadrature method, *Journal of Petroleum Science and Engineering*, **70**, 3-4, 235-242
6. Hannoyer M.J., Paidoussis M.P., 1978, Instabilities of tubular beams simultaneously subjected to internal and external axial flows, *Journal of Mechanical Design*, **100**, 328-336
7. Jin J.D., Song Z.Y., 2005, Parametric resonances of supported pipes conveying pulsating fluid, *Journal of Fluids and Structures*, **20**, 763-783
8. Lian Z.H., Zhang Q., Lin T.J., Wang F.H., 2015, Experimental and numerical study of drill string dynamics in gas drilling of horizontal wells, *Journal of Natural Gas Science and Engineering*, **27**, 3, 1412-1420
9. Luu T.P., 1983, On the dynamics of three systems involving tubular beams conveying fluid, M. Eng. Thesis, McGill University, Canada
10. Mongkolcheep K., Ruimi A., Palazzolo A., 2015, Modal reduction technique for predicting the onset of chaotic behavior due to lateral vibrations in drillstrings, *Journal of Vibration and Acoustics*, **137**, 2, 1-11
11. Navarro-López E.M., Cortés D., 2007, Avoiding harmful oscillations in a drillstring through dynamical analysis, *Journal of Sound and Vibration*, **307**, 152-171
12. NDRC, 2007, Practice for selection and use of drill pipe and drill collar (SY/T 6288-2007) (in Chinese), Petroleum Industry Press, Beijing
13. Ni Q., Wang Y.K., Tang M., Luo Y.Y., Yan H., Wang L., 2015, Nonlinear impacting oscillations of a fluid-conveying pipe subjected to distributed motion constraints, *Nonlinear Dynamics*, **81**, 893-906
14. Paidoussis M.P., 1973, Dynamics of cylindrical structures subjected to axial flow, *Journal of Sound and Vibration*, **29**, 3, 365-385
15. Paidoussis M.P., Luu T.P., Prabhakar S., 2008, Dynamics of a long tubular cantilever conveying fluid downwards, which then flows upwards around the cantilever as a confined annular flow, *Journal of Fluids and Structures*, **24**, 111-128
16. Panda L.N., Kar R.C., 2007, Nonlinear dynamics of a pipe conveying pulsating fluid with parametric and internal resonances, *Nonlinear Dynamics*, **49**, 9-30
17. Qian Q., Wang L., Ni Q., 2008, Vibration and stability of vertical upward-fluid-conveying pipe immersed in rigid cylindrical channel, *Acta Mechanica Solida Sinica*, **21**, 431-440
18. Rinaldi S., Paidoussis M.P., 2012, Theory and experiments on the dynamics of a free-clamped cylinder in confined axial air-flow, *Journal of Fluids and Structures*, **28**, 167-179
19. Sahebkar S.M., Ghazavi M.R., Khadem S.E., Ghayesh M.H., 2011, Nonlinear vibration analysis of an axially moving drillstring system with time dependent axial load and axial velocity in inclined well, *Mechanism and Machine Theory*, **46**, 743-760

20. Samuel R., Yao D.P., 2013, Drillstring vibration with hole-enlarging tools: analysis and avoidance, *Journal of Energy Resources Technology*, **135**, 3, 1-13

21. Tikhonov V.S., Safronov A.I., 2011, Analysis of postbuckling drillstring vibrations in rotary drilling of extended-reach wells, *Journal of Energy Resources Technology*, **133**, 4, 043102-043109

22. Wang L., 2009, A further study on the non-linear dynamics of simply supported pipes conveying pulsating fluid, *International Journal of Non-Linear Mechanics*, **44**, 115-121

23. Xu J., Yang Q.B., 2006, Flow-induced internal resonances and mode exchange in horizontal cantilevered pipe conveying fluid, *Applied Mathematics and Mechanics*, **27**, 1, 943-951

24. Zamani S.M., Hassanzadeh-Tabrizi S.A., Sharifi H., 2016, Failure analysis of drill pipe: a review, *Engineering Failure Analysis*, **59**, 605-623

25. Zhang Q., Miska S., 2005, Effects of flow–pipe interaction on drill pipe buckling and dynamics, *Journal of Pressure Vessel Technology*, **127**, 129-136

26. Zhao M., Zhu X.Z., Wang C.L., 2014, Nonlinear dynamic analysis of drill string system for horizontal oil well with different positions of stabilizers, *Applied Mechanics and Materials*, **716-717**, 615-618

27. Zhu W.P., Di Q.F., 2011, Effect of prebent deflection on lateral vibration of stabilized drill collars, SPE-120455-PA

28. Zhu X.Z., He Y.D., Chen L., Yuan H.Q., 2012, Nonlinear dynamics analysis of a drillstring-bit-wellbore system for horizontal oil well, *Advanced Science Letters*, **16**, 13-19

Manuscript received October 10, 2016; accepted for print July 15, 2017